




Analyzing WSTP trend: a new method for global warming assessment

Esmail Heydari Alamdarloo · Ehsan Moradi ·
Mahsa Abdolshahnejad · Yalda Fatahi ·
Hassan Khosravi  · Alexandre Marco da Silva

Received: 21 April 2021 / Accepted: 5 November 2021 / Published online: 15 November 2021
© The Author(s), under exclusive licence to Springer Nature Switzerland AG 2021

Abstract This paper tries to introduce a time-series of temperature parameters as a potential method for studying the global warming. So, we investigated the spatial–temporal variations of warm-season temperature parameters (WSTP), including *start time*, *end time*, *length of season*, *base value*, *peak time*, *peak value*, *amplitude*, *large integrated value*, *right drive*, and *left drive*, using a database of 30 years' period in different climates of Iran. We used daily temperature data from 1989 to 2018 over Iran to extract the parameters by TIMESAT software. We studied the trend analysis of WSTP through the Mann–Kendall method. Then, we considered the Pearson correlation coefficient to calculate the correlation between WSTP and time. We assessed the trends of the slope using a simple linear regression method. Then, we compared the results of the WSTP trend analysis in climatic zones. Our results accused the hyper-arid climatic zone has the longest warm season (194.89 days a year). The warm season in this region starts earlier than other regions and increases with moderate

speed (left drive, $0.19\text{ }^{\circ}\text{C day}^{-1}$). Then, it reaches a peak value ($31.3\text{ }^{\circ}\text{C}$) earlier than the different climatic zones. On the other hand, the humid regions' warm season starts with the shortest *length* and ends later than the other climatic zones (112.1 and 297.5 days a year for start and end times, respectively). We detected that the trend of the start time parameter has decreased by 98.02% of the study area during the last 30 years. The base value, length, and large integrated value parameters have an increasing trend of 66.47%, 80.11%, and 92.95% in Iran. The highest correlation coefficient with time was for start time and large integrated value parameters. Hence, the start time and large integrated value parameters have almost the most negative (< -0.5) and positive (> 5) trend slope, among other parameters, respectively. In general, these results demonstrate that the studied region has faced global warming impacts over time by increasing the warm season and thermal energy, especially in arid and hyper-arid. We highlight the necessity of planning the land use under the high natural vulnerability of the studied local, especially in this new age of global warming.

E. Heydari Alamdarloo · E. Moradi · M. Abdolshahnejad ·
Y. Fatahi · H. Khosravi (✉)
Department of Arid and Mountainous Regions
Reclamation, Faculty of Natural Resources, University
of Tehran, Tehran, Iran
e-mail: hakhosravi@ut.ac.ir

A. M. da Silva
Department of Environmental Engineering, Institute
of Sciences and Technology of Sorocaba, São Paulo State
University (UNESP), Sorocaba, SP, Brazil

Keywords Spatial–temporal variations of WSTP ·
TIMESAT · Mann–Kendall · Pearson correlation
coefficient · Simple linear regression

Introduction

In recent decades, climate change and global warming problems have raised concerns of planners and the researcher community and have increased the studies about the effect of these events (Kousari & Asadi Zarch, 2011). Researches have demonstrated that climate change has broad impacts on human health and security, water resources quantitative and qualitative, and food security that are crucial for human life (IPCC, 2007; Ahmad et al., 2020). Reasons that have increased global warming include industrialization and increased use of fossil fuels; moreover, developing some activities such as land-use change and degradation of forest have caused rising greenhouse gas emissions (Amiri & Eslamian, 2009; Jiang et al., 2020). Global warming has raised the frequency and severity of extremes temperatures (Khan et al., 2019). Human-made activities or natural processes have increased the temperature mean (Viola et al., 2010). IPCC¹ has reported that the average surface temperature warmed by 0.85 °C (0.65–1.06 °C) globally during 1880–2012 (Ghasemi, 2015).

Moreover, based on the atmospheric forecasting models, the earth's temperature will rise from 1 to 3.5 °C by 2100 (Amiri & Eslamian, 2010). The spatial and temporal variation trends of temperature show a common warming trend in the average temperature at the global level (Vose et al., 2005; Brown et al., 2008). Global warming and increasing the earth's atmosphere temperature have raised the evaporation process. Furthermore, in some regions far from the water bodies, the soil humidity and dried out plants caused some changes in runoff characteristics, groundwater level, and water cycle (Khosravi et al., 2015; Patil et al., 2020). Following the aforementioned destructive effect, an assessment of the variation and fluctuation of temperature is necessary. Due to the geographical location of the Middle East and its huge part located in an arid and semi-arid area, it has become one of the most vulnerable areas to climate change in forthcoming (IPCC, 2007; Kousari et al., 2013). Temperature fluctuations in some parts of Iran have been subjected to various investigations in recent decades.

Some researchers have considered different parameters to study the climate change in Iran as following: exploring the trends in minimum, maximum, and average temperatures; relative humidity; and precipitation using Kendall's rank correlation (Kousari & Asadi Zarch, 2011) and variability of extreme temperature and precipitation using a linear test analysis and Mann–Kendall test (Rahimzadeh et al., 2009); investigating of rainfall and mean annual of temperature trends by the Mann–Kendall test (Ghahraman, 2007; Modarres & da Silva, 2007); detecting trends of the time series of yearly of Tmax, Tmin, Tmean, annual and seasonal precipitation using Mann–Kendall, Mann–Whitney, and Mann–Kendall rank methods (Tabari et al., 2011); and discovering trends and spatial and temporal changes in rainfall and temperature variables using Mann–Kendall and Sen's slope estimator statistical tests (Mekonen & Berlie, 2020).

There are parametric and nonparametric techniques to study the trends (He, 2014). Parametric methods are more powerful and flexible than nonparametric methods. In contrast, nonparametric approaches are appropriate for abnormal distribution (Hess et al., 2001; Sharif et al., 2010). As a nonparametric technique, Mann–Kendall is mainly used to investigate the time series trend (Mann, 1945; Kendall, 1975; Dixon et al., 2006; You et al., 2016; Latif et al., 2020). The main strength of Mann–Kendall is related to handling missing and outliers data (Hamed, 2008; Khaliq et al., 2009). Many researchers have applied Mann–Kendall as the primary method to study the trend in climate and hydrologic variability studies worldwide (Douglas et al., 2000; Burns et al., 2007; Fengjin & Lianchun, 2011; Croitoru et al., 2012; Chakravarty & Kumar, 2020). Among the parametric methods, simple linear regression is one of the most helpful statistical approaches to determine the correlation of variables using correlation coefficient-*R*, as a linear relationship among dependent and independent variables (Mcbean & Motiee, 2008; Lamchin et al., 2018). Pearson's correlation is another method to evaluate the relationship between two parameters. In a study in Iran, Fathian et al. (2015) used this method for detecting the correlation between temperature and precipitation. In another study in Spain, El Kenawy et al. (2012) applied the Pearson correlation coefficient to investigate the relationships between meteorological parameters. According to previous studies, most of them chiefly emphasized determining the changing trend

¹ - International Panel on Climate Change.

based on climatic parameters. However, there have been few studies on the seasonal parameters of temperature in Iran and the world. For instance, Dammo et al. (2015) reported during 1981–2010 a rising trend of the annual and seasonal temperature over North-Eastern Nigeria. Meshram et al. (2020) analyzed the trend of temperature to assess the effects of climate change in the period of 1901–2016 in the Chhattisgarh State. Their results showed that the annual and seasonal temperature and entire stations had a rising trend during this period. Also, some studies in Iran include Zarenistanak et al. (2014) who have evaluated the trends and projections of temperature in the southwest region of Iran. Their results presented that the winter compared with other seasons was constant, and the indicator of Tmax was more consistent than Tmin and Tmean. Their results also showed that the higher amounts of temperatures in summer might rise than other season's temperatures. Ahmadi et al. (2018) calculated the spatial and temporal temperature in Iran. They found the seasonal and annual temperature had increasing trends in the whole country within the last half-century. Fallah-Ghalhari et al. (2019) identified Tmax and Tmin in Iran from 1976 through 2005; they reported the northwest part of Iran will experience increasing in the highest temperature. Also, they found the function of probability density for two parameters would be transferred to warmer temperatures. Besides, Miri et al. (2021) reported a rising trend of overall temperature seasons in most regions of Iran in the future. Their results also revealed that the most spatiotemporal variation of temperature is principally related to the mountain parts in the winter months and partially in the fall.

According to some of the published researches, application of time-series of satellite images using TIMESAT such as season start, beginning growing season, determining the classes of land cover, and monitoring the land surface has been studied (Eklundh & Jönsson, 2016; Parece & Campbell, 2018; Rihan et al., 2021), but limited evidence has been published about spatial–temporal variations of warm-season temperature parameters.

Some studies show that most researchers focus on the trend of temperature changes and have not paid attention to issues such as evaluating the trend of seasonal temperature parameters, including the time of start and end of the warm season, maximum

temperature, rate of temperature growth at the beginning of the warm season and rate of temperature decrease at the end of the warm season. These are necessary to understand better the phenomenon of global warming on the one hand and planning from macro to micro-based on sustainable development in various sectors (such as calculating water demand in agriculture). In the present study, for the first time in Iran as a novelty, an attempt has been made to calculate the main parameters for the warm season, including the cases mentioned, using daily temperature changes over 30 years, using TIMESAT software. Generally, the outstanding innovation of this study is the use of extracted warm-season temperature parameters and the analysis of their trend in different climatic zones of Iran.

Since the investigation of time-series of temperature parameters gives more comprehensive information about changing on spatial and temporal of warm season, therefore, the main goals of this study are (i) to detect the trend of WSTP using Mann–Kendall method, (ii) to calculate the correlation between WSTP and time with the Pearson correlation coefficient, (iii) to apply the simple linear regression method to assessment trends slope, and (iv) to compare the results of trends analysis of WSTP in the climatic zones.

Material and methods

Study area

Iran is located in southwest Asia between 25° 3' and 39° 47' north latitudes and between 44° 14' and 63° 20' east longitudes where approximately 81.8 million people live there. Iran covers an area of 1.648 million km² (Fig. 1). Alborz and Zagros mountain ranges, stretching in the northwest-northeast and northwest-southeast directions, respectively. Two long coastlines in the north (Caspian Sea) and south (Oman Sea and the Persian Gulf) and two central deserts, Kavir and Lut (in the central-east and central-north), are the leading topographical features of the country (Hadipour et al., 2019). The Zagros and Alborz mountains are the main reason for having a different climate in Iran (Heydari Alamdarloo et al., 2018). Most of Iran is located in arid and semi-arid climates with low precipitation and high evapotranspiration

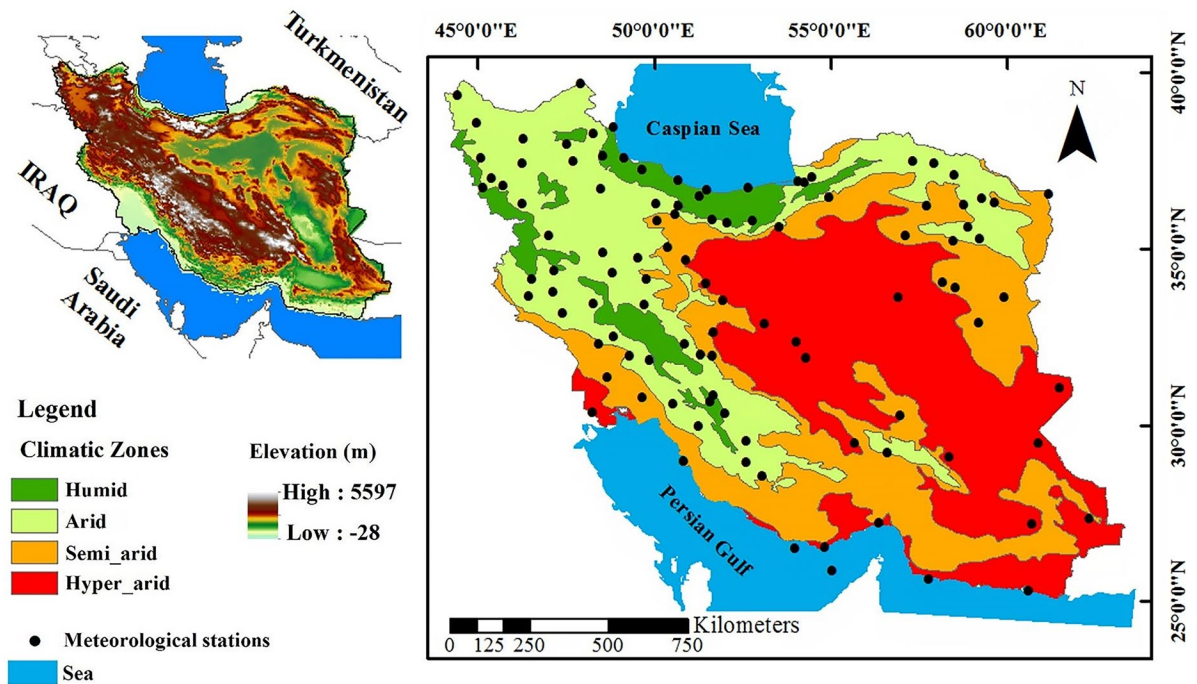


Fig. 1 Geographical location, topographic, and climatic classification maps of Iran

(Khalili et al., 2016; Fallah et al., 2017; Moradi et al., 2020). Mean annual precipitation varies from zero in the southern and eastern parts to $2000 \text{ mm/year}^{-1}$ in the Caspian Sea coastal areas. The average value of the mentioned variable over the entire country is about 250 mm year^{-1} . The mean annual temperature is another variable that varies from 10 in the west to $35 \text{ }^\circ\text{C}$ in the center (Mianabadi et al., 2018).

Data collection

In this study to investigate the changes in temperature trends, a set of daily temperature data of 103 meteorological stations from 1989 to 2018 was collected from the Iranian Meteorological Organization (<http://www.irimo.ir/>). Due to the data limitations, it was tried to use all available data at the stations. Finally, the information was prepared to analyze using TIME-SAT 3.3 software. Since some stations had missing data due to the different establishment times, the data set was investigated after a statistical defects survey for restoring lost data.

The focal point of this study lies in analyzing the temperature parameter trends of warm season in

Iran's climates during the studied period. In that case, the climatic classification map was obtained from the Forests, Range, and Watershed Management Organization of Iran (<http://www.frw.ir/02/En/default.aspx>) based on Domarten climate classification. To achieve the best result, some classes were merged, and some climatic zones are different. According to this map, Iran is divided into other climatic categories. The current study was performed in four climatic zones, including humid, arid, semi-arid, and hyper-arid (Behrang Manesh et al., 2019).

Extracting WSTP

WSTP was considered to analyze the temperature trend changes. Seasonality parameters have the potential to map out spatial or temporal changes in the temperature trends. The parameters shown in Fig. 2 were extracted from 30-year daily temperature time-series (Eklundh & Jönsson, 2017). Due to this fact that time-series, including a period of “n” years, have only “n–1” full seasons, so 29 full warm seasons with proper functions were identified.

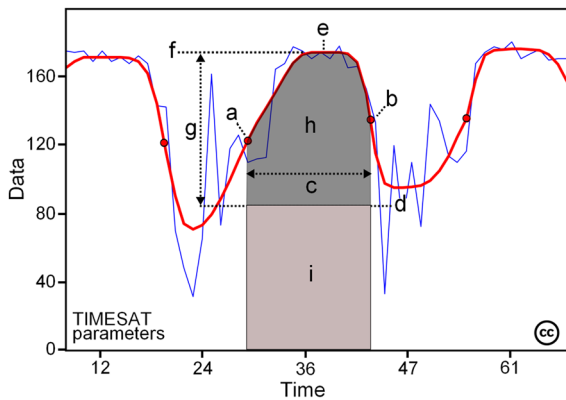


Fig. 2 WSTP: (a) start time, (b) end time, (c) length of season, (d) base value, (e) peak time, (f) peak value, (g) amplitude, (h) small integrated value, and (h+i) large integrated value. Filtered and original data are indicated by red and blue lines, respectively (Eklundh & Jönsson, 2017)

Figure 2 is an example for extracting the WSTP (warm-season temperature parameters) in a warm season of a spatial year using TIMESAT. The X-axis shows days around the warm season of the year. In this study, WSTP, like this figure, was extracted for all study years (1989–2018) in each station. The output included the WSTP 29 values (1989–2018) of “start time” in each station. Using interpolation of the WSTP, for example, start time,” the raster maps have been made. Then the statistical analysis was done on the raster maps series. According to Fig. 2, the start time (a) and the end time (b) of the season occurred when the left side of the curve and the right side of the curve reached a user defined level (often a certain fraction of the seasonal amplitude), respectively. Length of the season (c) refers to a time from the start to the end. The average of the left and right minimum values is known as a base value (d). Time for the middle of the season (e) is defined as a mean value of the times for which the left edge and the right edge have decreased to the 80% level. The most significant value for the fitted function during the season is named peak value (f); this is the maximum value of the season that may occur at different times in comparison with the middle of the season (Eklundh & Jönsson, 2017). Seasonal amplitude (g) is the difference between the maximum value and the base level. The parameters of (a), (b), (c), and (e) are in Julian Day Number (JDN), and parameters of (d), (f), and

(g) are in degree centigrade ($^{\circ}\text{C}$). The increase rate at the beginning of the season (left drive, in $^{\circ}\text{C day}^{-1}$) is the ratio of the difference between the left 20% and 80% levels. The corresponding time difference and the absolute value of this parameter named right drive ($^{\circ}\text{C day}^{-1}$) is the rate of decrease at the end of the season. Integral of the difference between the function describing the season and the base level from season start to season end was considered as a small seasonal integral (h). Large seasonal integral (h+i) is integral to the function describing the season from the season start to the season end. When part of the fitted function is negative, the large integral is meaningless. Values of the function at the start and end times of the season are value for the start of the season, and value for the end of the season, respectively (Eklundh & Jönsson, 2017).

TIMESAT software was used to provide a complete analysis of the mentioned parameters. Smoothing time series at each pixel is one of the essential steps in analyzing the seasonal parameters. The latest one was selected to smooth time-series in the TIMESAT package, among double logistic, asymmetric Gaussian, and Savitzky–Golay. The Savitzky–Golay method smoothly follows within-season variations and therefore captures subtle dynamics during the season. The mentioned method filters the noises through a quadratic polynomial, and the equation coefficients are calculated by weighted least square (Eklundh & Jönsson, 2015). After smoothing, the relative amplitude method was used to define the start and end of the warm season. The raster maps of WSTP for each warm season were created to investigate the trend changes using the inverse distance weighting (IDW) interpolation method in ArcGIS 10.3 software. Then, descriptive statistics, including mean and standard deviation of all these 10-seasonal temperature parameters, were calculated by the mentioned software for each warm season (10×29 raster maps).

Trend analysis using Mann–Kendall

The MK method was used to evaluate the WSTP trend over 29 seasons. We used standardized test statistic Z_c by calculating test statistics S and $\text{Var}(S)$ in this method. The equation for computing the test statistic S is given as Eq. (1):

$$S = \sum_{i=1}^{n-1} \sum_{j=i+1}^n \text{Sign}(x_j - x_i) \tag{1}$$

where (n) is the length of the dataset, (X_j) and (X_i) are the sequential data values esteem on occasion (j) and (i), and the sign means the sign capacity that takes on the values 1, 0, or -1 , if $X_j > X_i$, $X_j = X_i$ or $X_j < X_i$, respectively.

The variance statistic can be obtained as follow:

$$\text{Var}(S) = \frac{1}{18} \left[n(n-1)(2n+5) - \sum_p^q t_p(t_{p-1})(2t_p+5) \right] \tag{2}$$

In which (n) is the number of data points, (t_p) is the number of ties for p^{th} value, and (q) is the number of tied groups.

The test statistic Z_c has been calculated by the Eq. (3).

$$Z_c = \begin{cases} \frac{S-1}{\sqrt{\text{Var}(S)}}, S > 0 \\ 0, S = 0 \\ \frac{S-1}{\sqrt{\text{Var}(S)}}, S < 0 \end{cases} \tag{3}$$

The positive and value of Z_c show an increasing trend, and a negative value indicates a decreasing trend.

In the present study, to display changes in WSTP, Z_c values were applied. Then detailed maps of these extracted values by the Mann–Kendall method were prepared for each parameter. At the 5% significance level, the null hypothesis is rejected, and the time series of each parameter has a significant trend if the absolute value of Z_c is higher than 1.96. Otherwise, time-series data has no trend (Zhou et al., 2018). The Mann–Kendall coefficient was calculated for parameters by eliminating the seasonal trend from the data using Earth Trends Modeler (ETM) in TerrSet 18.31 software.

Trend analysis WSTP using Pearson’s correlation and linear regression

Furthermore, the Pearson correlation and simple linear regression were determined on the raster layers of WSTP using the TerrSet software to evaluate trends during the studied period. The equation to calculate the Pearson correlation coefficient (CC) or (r) is given as Eq. (4). In this equation, \bar{x} and \bar{y} are the average

of the first and the second dataset, respectively (Lee Rodgers & Nicewander, 1988; Kumar & Kaur, 2012).

$$r = \frac{\sum_{i=1}^n (x_i - \bar{x})(y_i - \bar{y})}{\sqrt{\sum_{i=1}^n (x_i - \bar{x})^2 \sum_{i=1}^n (y_i - \bar{y})^2}} \tag{4}$$

The Pearson correlation coefficient (r) value varies between 1 and -1 , which $+1$, zero, and -1 revealed a complete positive correlation, no correlation, and a complete negative correlation, respectively. In this study, the relationship between time and each of 10 seasonal parameters was calculated. The mean value of coefficient (r) was classified as maps in ArcGIS 10.3 software to accurately evaluate.

Trend analysis WSTP using linear regression

Simple linear regression (Rencher, 2002) was another approach to studying the linear relationship between dependent and independent variables. Here, the seasonal parameters and time were the dependent and independent variables, respectively. The slope coefficient of the regression line was calculated to evaluate the correlation between these variables according to Eq. (5) (Chatfield, 2016).

$$\text{Slope} = \frac{29 \left(\sum_{i=1988}^{2018} t_i y_i \right) - \left(\sum_{i=1988}^{2018} t_i \right) \left(\sum_{i=1988}^{2018} y_i \right)}{29 \sum_{i=1988}^{2018} t_i^2 - \left(29 \sum_{i=1988}^{2018} t_i \right)^2} \tag{5}$$

In this equation, (t) and (y) refer to time and seasonal parameters, respectively. It is important to note that the negative slope represents an inverse relationship. The positive slope indicates a direct connection, and the slope value shows the degree of dependence of the variables. The slope values were classified in ArcGIS 10.3 software to investigate the trends.

Results and discussion

WSTP

Table 1 indicates descriptive statistics of WSTP all over Iran. This table presents the mean and standard deviation (SD) values of seasonality parameters in four climatic zones for 29 warm seasons. According

Table 1 Descriptive statistics of WSTP in the study area

Climatic zones		Start time (day)		End time (day)		Length (day)		Peak time (°C)		Base value (°C)	
	Mean	SD	Mean	SD	Mean	SD	Mean	SD	Mean	SD	
Humid	112.1	4.56	297.55	2.02	185.48	4.66	206.89	2.03	3.81	2.93	
Semi-arid	107.91	4.28	296.33	2.24	188.41	4.81	204.44	3.09	3.02	3.61	
Arid	102.81	4.17	296.87	4.29	194.05	5.82	200.84	3.75	8.62	4.93	
Hyper-arid	100.8	4.1	295.69	3.92	194.89	6.12	199.09	3.3	8.3	4.05	
Climatic zones		Peak value (°C)		Amplitude (°C)		Left drive		Right drive		Large integrated	
	Mean	SD	Mean	SD	Mean	SD	Mean	SD	Mean	SD	
Humid	27.24	2.39	23.28	2.09	0.19	0.01	0.22	0.02	4346.79	427.32	
Semi-arid	27.38	2.92	24.21	1.47	0.2	0.01	0.22	0.02	4416.57	580.97	
Arid	30.78	2.6	22.04	3.12	0.19	0.02	0.2	0.03	5332.21	702.86	
Hyper-arid	31.27	1.8	22.85	3.11	0.19	0.02	0.2	0.03	5417.93	547.85	

to Table 1, WSTP in the climatic zones of Iran has various values. So that, the warm season starts earlier in the hyper-arid regions and ends earlier (100.8 and 295.69 days for *start* and *end times*, respectively). Also, it starts and ends later in the humid areas than other climatic zones (112.1 and 297.55 days for *start* and *end times*, respectively). On average, the difference between the start time of the warm seasons (11.3 days) is more than the end time of the warm season (1.86 days) in different climates in Iran, from humid toward hyper-arid.

According to Table 1, the average of rising temperature or warming rate at the beginning of the warm season (*left drive*) and lowering the temperature or cooling rate at the end of the warm season (*right drive*) are 0.01 and 0.02 (°C.day⁻¹), respectively in all climates.

Generally, both hyper-arid and humid climates are very noticeable. The hyper-arid climatic zone has the longest warm season (194.89 days a year), so that the warm season in this region starts earlier than other regions and increases with moderate speed (*left drive*, 0.19). Then, it reaches a *peak value* (31.27 °C) earlier than the different climatic zones. On the contrary, the humid climatic zone has the shortest warm season (185.48 days a year). So, it starts later than other climates and reaches a *peak value* (27.24 °C) with moderate speed (*left drive*, 0.19). The end of the warm season in humid regions occurs later than in other regions. Considering Table 1, the *peak value* of temperature in the humid zone is the lowest value among different climates.

According to the values of the *large integrated* parameter as a thermal energy index, it can be seen that the highest and lowest amounts of thermal energy index belong to the hyper-arid and humid regions, respectively. It is because of the longer length of the warm season and higher peak temperature in hyper-arid and the shortest length of warm season and lower peak temperature in humid regions. Since thermal properties play an essential role in plant development and growth (Iqbal et al., 2016), so the ecosystems of these climates are different.

The use of WSTP extracted from TIMESAT software to study temperature changes in Iran showed valuable results. The study of temperature changes in detail using seasonal temperature parameters such as season shovels, season length, end of the season, speed of temperature changes, and thermal energy has

been an innovation that has been used in this study. A review of previous investigations shows that the use of seasonal parameters used by TIMESAT software in other studies such as Guo et al. (2014), Parece and Campbell (2018), and Klein et al. (2021) has also been satisfactory. These studies applied TIMSAT to evaluate the urban phenology using thermal islands changes (Parece & Campbell, 2018), vegetation phenology using NDVI changes (Guo et al., 2014), and analysis of temporal-spatial changes surface water resource’s extension by time series of MODIS data set (Klein et al., 2021).

Extraction of seasonal parameters such as the beginning of the growing season, end of the growing season, start and end time, and length of spatial changes of water resources using the mentioned software is an example of studies that show the application of seasonal parameters that are consistent with the results of this study, and the use of this method further confirms the work. In all these studies, climate

change and global warming have affected water resources and vegetation as well as heat islands and caused changes in seasonal parameters. What makes the results of these studies more accurate is the use of seasonal parameters extracted from TIMESAT software. It should be noted that some parameters such as the rate of increase or decrease in temperature at the beginning and end of the warm season have been less considered by researchers and this research is one of the first studies in this field, so there is a need for more research in this subject.

Results of Mann–Kendall analysis

In Fig. 3, the trend of positive (increasing), negative (decreasing), and non-existent trends in the WSTP can be observed by Zc classification. Also, the area percentage of Iran’s climatic zones was shown to assess the WSTP trend using Zc classification in Table 2. During the last 30 years, the trend of the start

Fig. 3 Classification of the test statistic Zc (significance at the 5% level) to trend detection in WSTP during the study period

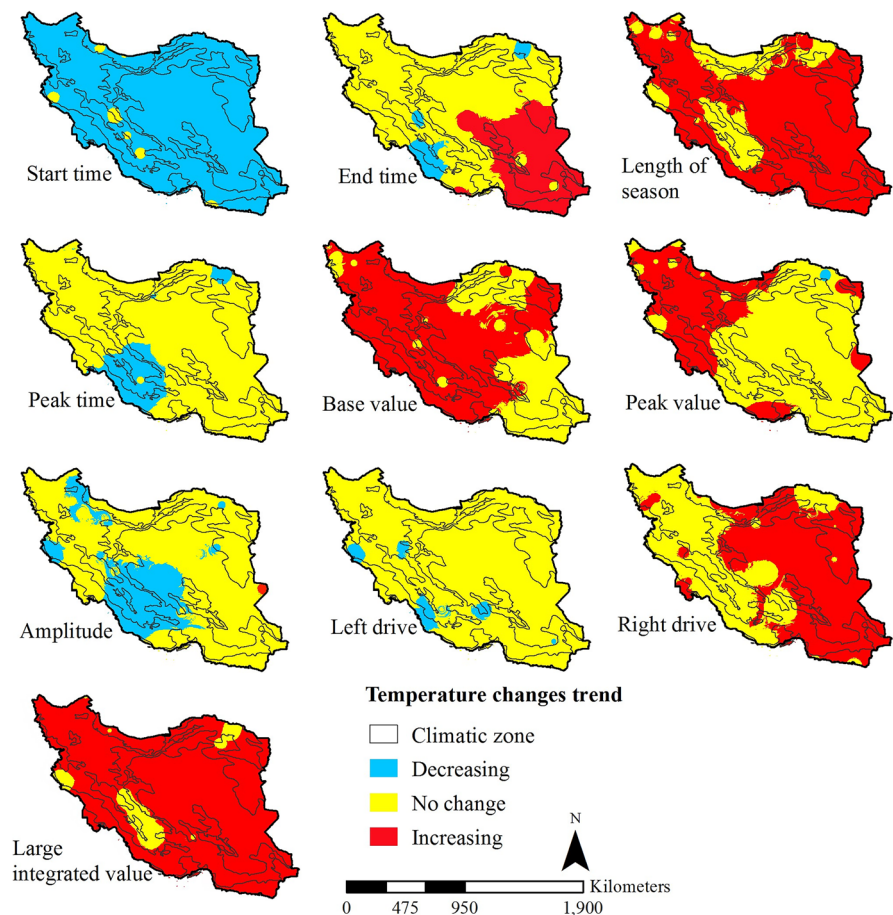


Table 2 The area percentage of Iran’s climatic zones for changes in WSTP using Zc classification

WSTP	Humid			Semi-arid			Arid			Hyper-Arid			Total
	–	no	+	–	no	+	–	no	+	–	no	+	
Start time	6.5	0.62	0	27.64	1.04	0	28.5	0.18	0	35.38	0.14	0	100
End time	0.4	6.73	0	2.63	25.46	0.6	1.54	18.2	8.94	0	18.03	17.47	100
Length	0	4.16	2.97	0	10.22	18.46	0	4.23	24.44	0	1.28	34.24	100
Peak time	0.48	6.65	0	5.49	23.19	0	3.83	24.84	0	1.28	34.24	0	100
Base value	0	0.81	6.31	0	5.1	23.58	0	11.12	17.56	0	16.5	19.02	100
Peak value	0	1.48	5.65	0.3	12.18	16.19	0.03	22.32	6.33	0	31.33	4.19	100
Amplitude	1.41	5.72	0	8.83	19.84	0	6.18	22.5	0	5.69	29.53	0.3	100
Left drive	0.06	7.07	0	2.18	26.51	0	1.83	26.83	0	0.31	35.21	0	100
Right drive	0	4.85	2.28	0	22.87	5.81	0	10.55	18.13	0	4.45	31.06	100
Large integrated	0	0.86	6.28	0	4.88	23.8	0	1.25	27.42	0	0.06	35.45	100

time parameter is decreasing in 98.02% of the study area. Base value, length, and large integrated have an increasing trend of 66.47%, 80.11%, and 92.95% of Iran, respectively. In Fig. 3 and Table 2, it is observed that the trends of four parameters include end time, peak time, amplitude, and left drive remained unchanged in most areas of Iran (68.42%, 88.92%, 77.59%, and 95.62% of Iran, respectively).

According to Table 2, the start time parameter decreases in 6.5%, 27.64%, 28.5%, and 35.38% of humid, semi-arid, arid, and hyper-arid regions of Iran’s climatic zones. About the end time parameter, 6.73% of humid, 25.46% of semi-arid, 18.2% of arid, and 18.03% of hyper-arid regions have no change in trends. Besides, regarded as a positive trend in the length of season parameter, 2.97%, 18.46%, 24.44%, and 34.24% of humid, semi-arid, arid, and hyper-arid regions are increasing, respectively. The

area percentage of climatic zones for changes in other WSTP using Zc classification is observable in Table 2.

Peak value does not have any particular trend in most arid and hyper-arid regions. Still, it has an increasing trend, mostly in northwestern Iran, having a humid and semi-arid climate (Fig. 3). These results are consistent with Fallah-Ghalhari et al. (2019), who evaluated the impact of climate change on maximum and minimum temperatures in Iran. The base and peak value parameters have an increasing trend in some regions, so it can be concluded that the maximum and minimum temperatures are rising in these regions. Since increasing the maximum and minimum temperatures have more effects on the environment than the average temperature (Zhang et al., 2007), changes in the ecosystem of these regions can be considerable.

Table 3 Trend analysis of seasonal temperature parameters using the test statistic Zc in the study area

Climatic zones	WSTP					
	Start time Zc	End time Zc	Length Zc	Peak time Zc	Base value Zc	
Humid	-2.79*	-0.18	1.76	-1.17	2.71*	
Semi-arid	-3.12*	-0.32	2.03*	-1.38	2.46*	
Arid	-3.28*	0.91	2.59*	-1.04	2.12*	
Hyper-arid	-3.36*	1.67	2.96*	-0.58	1.81	
Climatic zones	Peak value Zc	Amplitude Zc	Left drive Zc	Right drive Zc	Large integrated Zc	
Humid	2.44*	-1.56	-0.59	1.64	2.68*	
Semi-arid	1.9	-1.7	-1.07	1.47	2.8*	
Arid	1.12	-1.33	-1.1	2.11*	3.04*	
Hyper-arid	0.93	-0.96	-0.98	2.41*	3.51*	

*Significance at the 5% level

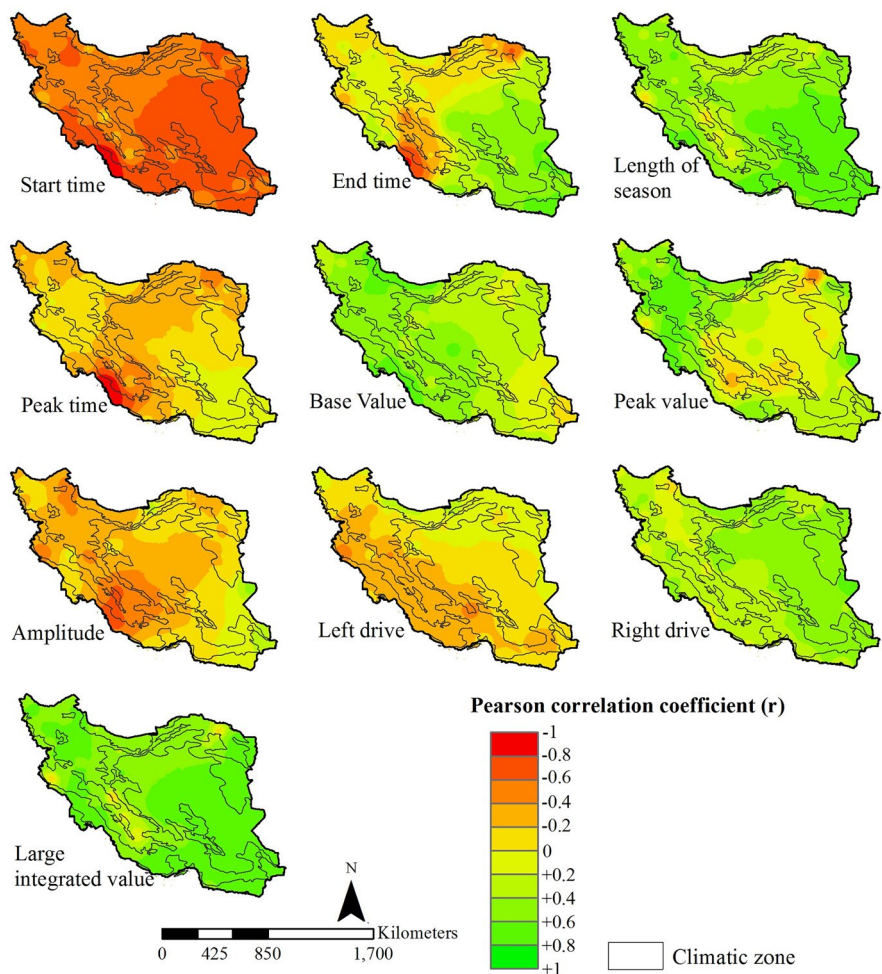
Table 4 The mean of Pearson correlation coefficient (*r*) and slope of a linear regression between WSTP and time

WSTP											
Climatic zones	Start time		End time		Length		Peak time		Base value		Slope
	<i>r</i>	Slope	<i>r</i>	Slope	<i>r</i>	Slope	<i>r</i>	Slope	<i>r</i>	Slope	
Humid	-0.51	-0.38	-0.05	-0.02	0.37	0.35	-0.2	-0.09	0.53	0.08	
Semi-arid	-0.56	-0.46	-0.06	-0.03	0.41	0.42	-0.25	-0.13	0.45	0.08	
Arid	-0.62	-0.51	0.2	0.07	0.54	0.58	-0.2	-0.10	0.35	0.04	
Hyper-arid	-0.63	-0.50	0.34	0.16	0.59	0.66	-0.12	-0.05	0.3	0.03	
Climatic zones	Peak value		Amplitude		Left drive		Right drive		Large integrated		Slope
	<i>r</i>	Slope	<i>r</i>	Slope	<i>r</i>	Slope	<i>r</i>	Slope	<i>r</i>	Slope	
Humid	0.47	0.04	-0.3	-0.04	-0.08	-0.0001	0.32	0.001	0.51	14.72	
Semi-arid	0.36	0.03	-0.31	-4.81	-0.16	-0.03	0.029	0.0009	0.52	15.35	
Arid	0.23	0.01	-0.2	-0.02	-0.16	-0.0003	0.4	0.001	0.6	20.40	
Hyper-arid	0.2	0.01	-0.15	-0.02	-0.1	-0.0002	0.44	0.0012	0.65	23.22	

There is a significant increase in the length of the warm season in all climatic zones except humid zones during 30 years. Since temperature plays a vital

role in drought (Vicente-Serrano et al., 2014), it is expected that Iran’s moist and semi-arid regions will become drier regions over time. It is consistent with

Fig. 4 Classification of Pearson correlation coefficient (*r*) during the studied period



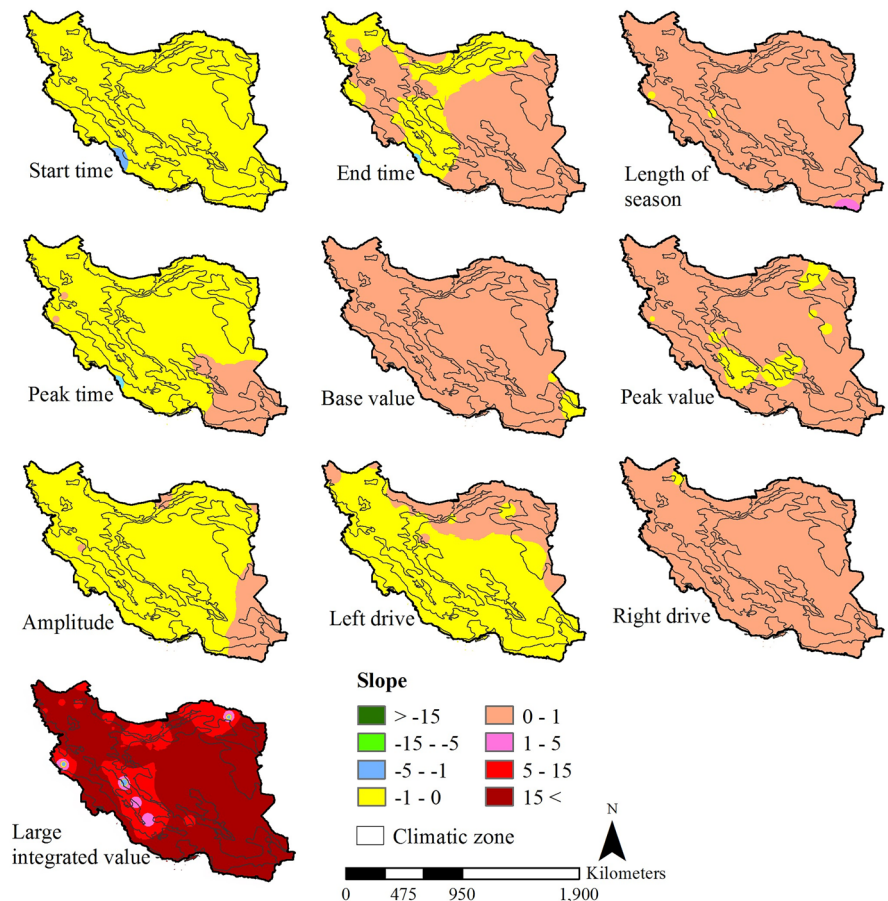
HadiPour et al. (2020), who point it out in a study addressing the spatial variability of drought index in dry regions of Iran. In general, it seems to be happening in other parts of the world (Li et al., 2019; Koutroulis, 2019). Increasing aridity will increase land degradation and reduce biodiversity in these areas (Durán et al., 2018). A remarkable fact is that although the base value and peak value are increasing, the amplitude trend is not significant in most climatic regions.

Table 3 indicates the values of the test statistic Z_c in climatic zones for WSTP at a significant 5% level. Regarding this table, the average Z_c value for start time and large integrated parameters in all climatic zones and length and base value parameters in more climatic zones is significant. The trend of start time is decreasing, and for base value, length, and large integrated is increasing. It means that the warm season starts earlier over time in almost all over Iran from 1989 to 2018 years. It has affected on length of the

season and, finally, the thermal energy index of the warm season (large integrated value). These results indicate warm season in Iran is changing, which can be a consequence of global warming (Shokoohi et al., 2014). Change of warm season impacts on plant growth (Roshan et al., 2014; Behrang Manesh et al., 2019) and land surface processes such as evapotranspiration (ET), sublimation from snow, and stream-flow (Das et al., 2011).

The Pearson correlation coefficient and linear regression were analyzed to determine the correlation between WSTP and time. The mean of Pearson correlation coefficient (r) and slope for linear regression is presented in Table 4. Regarding this table, the correlation coefficient for four parameters, including start time, peak time, amplitude, and left drive, decreases. Five parameters, including length of season, base value, peak value, right drive, and large integrated value, are increasing in most regions of the study area. The correlation coefficient for the end time

Fig. 5 The slope of the regression line between WSTP and time during the studied period



parameter increases in arid and hyper-arid climatic zones and decreases in humid and semi-arid regions.

According to Table 4, the *peak temperature value in humid and semi-arid regions correlates with time more than in hyper-arid and arid areas*. The correlation coefficient increases moving toward the northwest of this region. Also, the slope of changes for this parameter shows a high average in humid and semi-arid regions. This result follows Mahmoudi et al. (2019), who evaluated the temperature change trends in Iran. Having essential roles in agriculture and ecosystem (Leng et al., 2015; Liu et al., 2017), with increasing the peak and base temperature in humid and semi-arid regions, food security in these regions will generally face problems in the future.

Figure 4 shows the average Pearson correlation coefficient (r) in climatic zones between the WSTP and time. According to Fig. 4, the highest correlation coefficient is for start time and large integrated value parameters. Analysis of linear regression shows that the parameters of the start time, peak time, amplitude, and left drive have a decreasing slope in all climatic regions of Iran. As shown in Fig. 5 and Table 4, start time and large integrated value parameters have almost the most negative (< -0.5) and positive (> 5) trend slope among other parameters, respectively. Also, *the left drive and Right drive have the least negative and positive trend slope among other parameters*. The slope coefficient classification (Fig. 5) shows that more parameters range between 1 and -1 , except large integrated value. Generally, although the start time of warm-season decreases in slope between 0.38 and 0.51, the thermal energy index (large integrated value) increases with a slope of more than 14. This result demonstrates we face global warming in Iran. According to Smadi (2006), the changing temperature trends are due to increasing greenhouse gases and urbanization, and global warming. Overall, the increasing temperature in Iran will lead to increasing potential evapotranspiration, drought, and desertification (Tabari et al., 2011). It is a significant concern for scientists that impacts human life and the environment.

Conclusions

This study investigated the warm-season temperature parameters (WSTP) by using long-term trends in the

daily temperatures time series at 103 meteorological stations all over Iran from 1989 to 2018. The results of WSTP analysis showed that the most significant difference in WSTP values is between humid and hyper-arid climatic zones. Also, from drier to wetter regions, the length of the warm season and the peak temperature decrease. We demonstrated that air humidity in these climatic regions has the most important role in moderate air temperature. Evaluation of the long-term trend of WSTP indicated the warm-season thermal energy index influenced by the start time, season length, and base value of temperature more than other parameters. So, the large integrated value as the thermal energy index increases almost all over Iran.

Regarding the large integrated value of the warm season, we detected that the warm season in Iran is changing towards increasing the thermal energy index with the most positive slope (> 5). The hyper-arid region encompasses the most changes of the warm season since it has the most trend slope of thermal energy index (23.22) in this season. On the other hand, the humid zones are the regions with the lowest temperature changes (slope of significant integrated value, 14.72) in the warm season in Iran. These results demonstrate that Iran has faced global warming impacts over time. In general, warm-season change affects on the ecosystem, mainly arid and hyper-arid regions and causes degradation and desertification over time. The current investigation can be an alarm warning to humans for the reduction of abuse and exploitation on the environment, expansion of desertification, and degradation. Regarding the relationship between ecosystem and warm-season change, study of the effect of temperature parameters on the dynamic of vegetation cover will be an exciting study in future work.

Acknowledgements The authors are grateful to the Iran Meteorological Organization (IRIMO) for providing the meteorological data and the Forests, Range and Watershed Management Organization of Iran for giving the climatic map of Iran for this study.

Author contribution Formal analysis: EHA. Methodology: EHA, EM. Resources: MA, YF. Software: EHA, EM, YF. Supervision: HK. Writing—original draft: MA. Writing—review and editing: HK, AMdS.

Data availability All relevant data are within the manuscript.

Declarations

Conflict of interest The authors declare no competing interests.

References

- Ahmad, N., Shaffril, H. A. M., Samah, A. A., Idris, K., Samah, B. A., & Hamdan, M. E. (2020). The adaptation towards climate change impacts among islanders in Malaysia. *Science of The Total Environment*, 699, 134404.
- Ahmadi, F., Nazeri Tahroudi, M., Mirabbasi, R., Khalili, K., & Jhahharia, D. (2018). Spatiotemporal trend and abrupt change analysis of temperature in Iran. *Meteorological Applications*, 25(2), 314–321.
- Amiri, M. J., & Eslamian, S. S. (2009). Deficit irrigation is the way to improve water productivity in agriculture. Agriculture in Zagros region and adaptation for sustainable development. Yasoj Islamic Azad University.
- Amiri, M. J., & Eslamian, S. S. (2010). Investigation of climate change in Iran. *Journal of Environmental Science and Technology*, 3(4), 208–216.
- Behrang Manesh, M., Khosravi, H., Alamdarloo, E. H., Alekasir, M. S., Gholami, A., & Singh, V. P. (2019). Linkage of agricultural drought with meteorological drought in different climates of Iran. *Theoretical and Applied Climatology*, 1–9.
- Brown, S. J., Caesar, J., & Ferro, C. A. (2008). Global changes in extreme daily temperature since 1950. *Journal of Geophysical Research: Atmospheres*, 113(D5).
- Burns, D. A., Klaus, J., & McHale, M. R. (2007). Recent climate trends and implications for water resources in the Catskill Mountain region, New York, USA. *Journal of Hydrology*, 336(1–2), 155–170.
- Chakravarty, P., & Kumar, M. (2020). Mann-Kendall Trend analysis of weather parameters (1901–2002) of 4 districts with different land use pattern of Jharkhand during pre-monsoon period. *Studies in Indian Place Names*, 40(3), 2391–2404.
- Chatfield, C. (2016). *The analysis of time series: An introduction*. Chapman and Hall/CRC Press.
- Croitoru, A. E., Holobaca, I. H., Lazar, C., Moldovan, F., & Imbroane, A. (2012). Air temperature trend and the impact on winter wheat phenology in Romania. *Climatic Change*, 111(2), 393–410.
- Dammo, M. N., Abubakar, B. I., & Sangodoyin, A. Y. (2015). Trend and change analysis of monthly and seasonal temperature series over north-eastern Nigeria. *Journal of Geography, Environment and Earth Science International*, 3(2), 1–8.
- Das, T., Pierce, D. W., Cayan, D. R., Vano, J. A., & Lettenmaier, D. P. (2011). The importance of warm-season warming to western US streamflow changes. *Geophysical Research Letters*, 38(23).
- Dixon, H., Lawler, D. M., & Shamseldin, A. Y. (2006). Streamflow trends in western Britain. *Geophysical Research Letters*, 33(19).
- Douglas, E. M., Vogel, R. M., & Kroll, C. N. (2000). Trends in floods and low flows in the United States: Impact of spatial correlation. *Journal of Hydrology*, 240(1–2), 90–105.
- Durán, J., Delgado-Baquerizo, M., Dougill, A. J., Guuroh, R. T., Linstädter, A., Thomas, A. D., & Maestre, F. T. (2018). Temperature and aridity regulate spatial variability of soil multifunctionality in drylands across the globe. *Ecology*, 99(5), 1184–1193.
- Eklundh, L., & Jönsson, P. (2015). TIMESAT 3.2 with Parallel Processing Software Manual; Lund University. Lund, Sweden, 22–24.
- Eklundh, L., & Jönsson, P. (2016). TIMESAT for processing time-series data from satellite sensors for land surface monitoring. In *Multitemporal Remote Sensing* (pp. 177–194). Springer, Cham.
- Eklundh, L., & Jönsson, P. (2017). TIMESAT 3.2 with Parallel Processing Software Manual; Lund University. Lund, Sweden.
- El Kenawy, A., López-Moreno, J. I., & Vicente-Serrano, S. M. (2012). Trend and variability of surface air temperature in northeastern Spain (1920–2006): Linkage to atmospheric circulation. *Atmospheric Research*, 106, 159–180.
- Fallah, B., Sodoudi, S., Russo, E., Kirchner, I., & Cubasch, U. (2017). Towards modeling the regional rainfall changes over Iran due to the climate forcing of the past 6000 years. *Quaternary International*, 429, 119–128.
- Fallah-Ghalhari, G., Shakeri, F., & Dadashi-Roudbari, A. (2019). Impacts of climate changes on the maximum and minimum temperature in Iran. *Theoretical and Applied Climatology*, 138(3–4), 1539–1562.
- Fathian, F., Morid, S., & Kahya, E. (2015). Identification of trends in hydrological and climatic variables in Urmia Lake basin. *Iran. Theoretical and Applied Climatology*, 119(3–4), 443–464.
- Fengjin, X., & Lianchun, S. (2011). Analysis of extreme low-temperature events during the warm season in Northeast China. *Natural Hazards*, 58(3), 1333–1344.
- Ghahraman, B. (2007). Time trend in the mean annual temperature of Iran. *Turkish Journal of Agriculture and Forestry*, 30(6), 439–448.
- Ghasemi, A. R. (2015). Changes and trends in maximum, minimum and mean temperature series in Iran. *Atmospheric Science Letters*, 16(3), 366–372.
- Guo, W., Ni, X., Jing, D., & Li, S. (2014). Spatial-temporal patterns of vegetation dynamics and their relationships to climate variations in Qinghai Lake Basin using MODIS time-series data. *Journal of Geographical Sciences*, 24(6), 1009–1021.
- HadiPour, S., Wahab, A. K. A., & Shahid, S. (2020). Spatiotemporal changes in aridity and the shift of drylands in Iran. *Atmospheric Research*, 233, 104704.
- HadiPour, S., Wahab, A., Khairi, A., Shahid, S., & Wang, X. (2019). Spatial pattern of the unidirectional trends in thermal bioclimatic indicators in Iran. *Sustainability*, 11(8), 2287.
- Hamed, K. H. (2008). Trend detection in hydrologic data: The Mann-Kendall trend test under the scaling hypothesis. *Journal of Hydrology*, 349(3–4), 350–363.

- He, M. (2014). Water quantity and water quality trend analysis in northwest Indiana using modified Mann Kendall test (Doctoral dissertation, Purdue University).
- Hess, A., Iyer, H., & Malm, W. (2001). Linear trend analysis: A comparison of methods. *Atmospheric Environment*, 35(30), 5211–5222.
- Heydari Alamdarloo, E., Behrang Manesh, M., & Khosravi, H. (2018). Probability assessment of vegetation vulnerability to droughted based on remote sensing data. *Environmental Monitoring and Assessment*, 190(12), 702.
- Inter-Governmental Panel on Climate Change (IPCC). (2007). Climate change and agriculture in Africa: Impact assessment and adaptation strategies. <https://www.earthprint.com>
- Iqbal, M. A., Penas, A., Cano-Ortiz, A., Kersebaum, K. C., Herrero, L., & del Rfo, S. (2016). Analysis of recent changes in maximum and minimum temperatures in Pakistan. *Atmospheric Research*, 168, 234–249.
- Jiang, Q., Qi, Z., Xue, L., Bukovsky, M., Madramootoo, C. A., & Smith, W. (2020). Assessing climate change impacts on greenhouse gas emissions, N losses in drainage and crop production in a subsurface drained field. *Science of The Total Environment*, 705, 135969.
- Kendall, M. G. (1975). Rank correlation measures. *Charles Griffin, London*, 202, 15.
- Khalili, K., Nazeri Tahoudi, M., Mirabbasi, R., & Ahmadi, F. (2016). Investigation of spatial and temporal variability of precipitation in Iran over the last half century. *Stoch Environ Res Risk Assess*, 30(4), 1205–1221.
- Khaliq, M. N., Ouarda, T. B. M. J., Gachon, P., Sushama, L., & St-Hilaire, A. (2009). Identification of hydrological trends in the presence of serial and cross correlations: A review of selected methods and their application to annual flow regimes of Canadian rivers. *Journal of Hydrology*, 368(1–4), 117–130.
- Khan, N., Shahid, S., & bin Ismail, T., & Wang, X. J. (2019). Spatial distribution of unidirectional trends in temperature and temperature extremes in Pakistan. *Theoretical and Applied Climatology*, 136(3–4), 899–913.
- Klein, I., Mayr, S., Gessner, U., Hirner, A., & Kuenzer, C. (2021). Water and hydropower reservoirs: High temporal resolution time series derived from MODIS data to characterize seasonality and variability. *Remote Sensing of Environment*, 253, 112207.
- Khosravi, H., Moradi, E., & Darabi, H. (2015). Identification of homogeneous groundwater quality regions using factor and cluster analysis; A case study Ghir Plain of Fars Province. *Irrigation and Water Engineering*, 6(1), 119–133.
- Kousari, M. R., & Asadi Zarch, M. A. A. (2011). Minimum, maximum, and mean annual temperatures, relative humidity, and precipitation trends in arid and semi-arid regions of Iran. *Arabian Journal of Geosciences*, 4(5–6), 907–914.
- Kousari, M. R., Ahani, H., & Hendi-zadeh, R. (2013). Temporal and spatial trend detection of maximum air temperature in Iran during 1960–2005. *Global and Planetary Change*, 111, 97–110.
- Koutroulis, A. G. (2019). Dryland changes under different levels of global warming. *Science of the Total Environment*, 655, 482–511.
- Kumar, S., & Kaur, H. (2012). Face recognition techniques: Classification and comparisons. *International Journal of Information Technology and Knowledge Management*, 5(2), 361–363.
- Lamchin, M., Lee, W. K., Jeon, S. W., Wang, S. W., Lim, C. H., Song, C., & Sung, M. (2018). Long-term trend and correlation between vegetation greenness and climate variables in Asia based on satellite data. *Science of the Total Environment*, 618, 1089–1095.
- Latif, Y., Yaoming, M., Yaseen, M., Muhammad, S., & Wazir, M. A. (2020). Spatial analysis of temperature time series over the Upper Indus Basin (UIB) Pakistan. *Theoretical and Applied Climatology*, 139(1), 741–758.
- Lee Rodgers, J., & Nicewander, W. A. (1988). Thirteen ways to look at the correlation coefficient. *The American Statistician*, 42(1), 59–66.
- Leng, G., Tang, Q., & Rayburg, S. (2015). Climate change impacts on meteorological, agricultural and hydrological droughts in China. *Global and Planetary Change*, 126, 23–34.
- Li, Y., Chen, Y., & Li, Z. (2019). Dry/wet pattern changes in global dryland areas over the past six decades. *Global and Planetary Change*, 178, 184–192.
- Liu, S., Huang, S., Huang, Q., Xie, Y., Leng, G., Luan, J., & Li, X. (2017). Identification of the non-stationarity of extreme precipitation events and correlations with large-scale ocean-atmospheric circulation patterns: A case study in the Wei River Basin, China. *Journal of Hydrology*, 548, 184–195.
- Mahmoudi, P., Mohammadi, M., & Daneshmand, H. (2019). Investigating the trend of average changes of annual temperatures in Iran. *International Journal of Environmental Science and Technology*, 16(2), 1079–1092.
- Mann, H. B. (1945). Nonparametric tests against trend. *Econometrica: Journal of the Econometric Society*, 245–259.
- McBean, E., & Motiee, H. (2008). Assessment of impact of climate change on water resources: A long term analysis of the Great Lakes of North America. *Hydrology and Earth System Sciences Discussions, European Geosciences Union*, 12(1), 239–255.
- Mekonen, A. A., & Berlie, A. B. (2020). Spatiotemporal variability and trends of rainfall and temperature in the North-eastern Highlands of Ethiopia. *Modeling Earth Systems and Environment*, 6(1), 285–300.
- Meshram, S. G., Kahya, E., Meshram, C., Ghorbani, M. A., Ambade, B., & Mirabbasi, R. (2020). Long-term temperature trend analysis associated with agriculture crops. *Theoretical and Applied Climatology*, 140(3), 1139–1159.
- Mianabadi, A., Shirazi, P., Ghahraman, B., Coenders-Gerrits, A. M. J., Alizadeh, A., & Davary, K. (2018). Assessment of short- and long-term memory in trends of major climatic variables over Iran: 1966–2015. *Theoretical and Applied Climatology*, 135(1–2), 677–691.
- Miri, M., Samakosh, J. M., Razieli, T., Jalilian, A., & Mahmodi, M. (2021). Spatial and temporal variability of temperature in Iran for the twenty-first century foreseen by the CMIP5 GCM models. *Pure and Applied Geophysics*, 178(1), 169–184.
- Modarres, R., & da Silva, V. D. P. R. (2007). Rainfall trends in arid and semi-arid regions of Iran. *Journal of Arid Environments*, 70(2), 344–355.
- Moradi, E., Khosravi, H., Zehabian, G., Khalighi-Sigaroodi, S., & Cerda, A. (2020). Vulnerability assessment of land degradation using network analysis process and

- geographic information system (case study: Maharloo-Bakhtegan Watershed). *Iranian Journal of Soil and Water Research*, 51(5), 1069–1080.
- Parece, T. E., & Campbell, J. B. (2018). Intra-urban microclimate effects on phenology. *Urban Science*, 2(1), 26.
- Patil, N. S., Chetan, N. L., Nataraja, M., & Suthar, S. (2020). Climate change scenarios and its effect on groundwater level in the Hiranyakeshi watershed. *Groundwater for Sustainable Development*, 100323.
- Rahimzadeh, F., Asgari, A., & Fattahi, E. (2009). Variability of extreme temperature and precipitation in Iran during recent decades. *International Journal of Climatology: A Journal of the Royal Meteorological Society*, 29(3), 329–343.
- Rencher, A. C. (2002). *Methods of multivariate analysis* (2nd ed.). Wiley.
- Rihan, W., Zhang, H., Zhao, J., Shan, Y., Guo, X., Ying, H., & Li, H. (2021). Promote the advance of the start of the growing season from combined effects of climate change and wildfire. *Ecological Indicators*, 125, 107483.
- Roshan, G., Oji, R., & Al-Yahyai, S. (2014). Impact of climate change on the wheat-growing season over Iran. *Arabian Journal of Geosciences*, 7(8), 3217–3226.
- Sharif, M., Burn, D., & Hussain, A. (2010). Climate change impacts on extreme flow measures in Satluj River Basin in India. In *World Environmental and Water Resources Congress 2010: Challenges of Change* (pp. 46–59).
- Shokoohi, A. R., Raziie, T., & Daneshkar Arasteh, P. (2014). On the effects of climate change and global warming on water resources in Iran. *International Bulletin of Water Resources & Development*, 2(4), 1–9.
- Smadi, M. M. (2006). Observed abrupt changes in minimum and maximum temperatures in Jordan in the 20th century. *American Journal of Environmental Sciences*, 2(3), 114–120.
- Tabari, H., Somee, B., & Rezaeianzadeh, M. (2011). Testing for long-term trends in climatic variables in Iran. *Atmospheric Research*, 100(1), 132–140.
- Vicente-Serrano, S. M., Lopez-Moreno, J. I., Beguería, S., Lorenzo-Lacruz, J., Sanchez-Lorenzo, A., García-Ruiz, J. M., & Coelho, F. (2014). Evidence of increasing drought severity caused by temperature rise in southern Europe. *Environmental Research Letters*, 9(4), 044001.
- Viola, F. M., Paiva, S. L., & Savi, M. A. (2010). Analysis of the global warming dynamics from temperature time series. *Ecological Modelling*, 221(16), 1964–1978.
- Vose, R. S., Easterling, D. R., & Gleason, B. (2005). Maximum and minimum temperature trends for the globe: An update through 2004. *Geophysical Research Letters*, 32(23).
- You, Q., Min, J., & Kang, S. (2016). Rapid warming in the Tibetan Plateau from observations and CMIP5 models in recent decades. *International Journal of Climatology*, 36(6), 2660–2670.
- Zarenistanak, M., Dhorde, A. G., & Kripalani, R. H. (2014). Trend analysis and change point detection of annual and seasonal precipitation and temperature series over southwest Iran. *Journal of Earth System Science*, 123(2), 281–295.
- Zhang, Y., Xu, Y. L., Dong, W. J., & Cao, L. J. (2007). A preliminary analysis of distribution characteristics of maximum and minimum temperature and diurnal temperature range changes over China under SRES B2 scenario. *Chinese Journal of Geophysics*, 50(3), 632–642.
- Zhou, X., Huang, G., Wang, X., & Cheng, G. (2018). Future changes in precipitation extremes over Canada: Driving factors and inherent mechanism. *Journal of Geophysical Research: Atmospheres*, 123(11), 5783–5803.

Publisher’s Note Springer Nature remains neutral with regard to jurisdictional claims in published maps and institutional affiliations.